JACS
JOURNAL OF THE AMERICAN CHEMICAL SOCIETY
pubs.acs.org/JACS
Article

Photocatalytic Synthesis of Substituted 2-Aryl Morpholines via Diastereoselective Annulation

Tiffany A. Brisco, Simon De Kreijger, Vaishnavi N. Nair, Ludovic Troian-Gautier,* and Uttam K. Tambar*

Cite This: J. Am. Chem. Soc. 2025, 147, 14605−14613
Read Online
ACCESS | Metrics & More | Article Recommendations | Supporting Information

ABSTRACT: Morpholines are prevalent in medicinal chemistry due to their favorable pharmacokinetic properties and widespread presence in FDA-approved drugs. Existing methods for morpholine synthesis often require prefunctionalized or protected reagents, limiting their versatility and efficiency. Here, we present a photocatalytic, diastereoselective annulation strategy for the synthesis of morpholines directly from readily available starting materials. This method employs a visible-light-activated photocatalyst, Lewis acid, and Brønsted acid to achieve high yields and stereoselectivity. It also provides access to diverse substitution patterns, including challenging tri- and tetra-substituted morpholines. Mechanistic studies reveal that the reaction proceeds through the formation of a radical cation intermediate, with triflic acid playing critical roles in protonating the substrate, preserving the photocatalyst, and preventing product oxidation. Beyond morpholines, this strategy is extended to piperidines, pyrrolidines, and other privileged nitrogen heterocycles. Our findings provide a modular approach for constructing complex, medicinally valuable scaffolds, advancing both synthetic and medicinal chemistry.

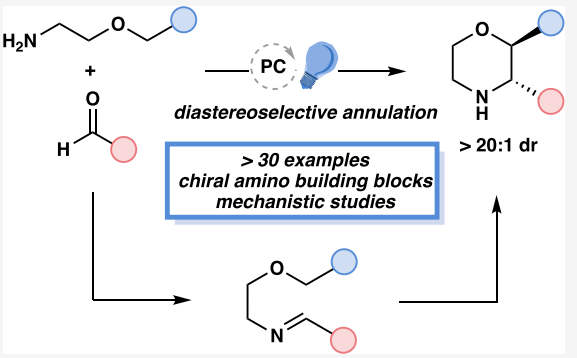

INTRODUCTION

N-heterocycles are present in more than 80% of the top 200 selling FDA approved drugs,[1,2] and new methods for their selective synthesis continue to be an important area of chemical research.[3,4] In this context, morpholines (**1**) confer many drug-like physical properties, such as favorable solubility, permeability, and stability, that have elevated them into the pantheon of medicinally valuable *N*-heterocycles (Figure 1a).[5] Most notably, their presence in molecules can lead to improved pharmacokinetic and metabolic profiles as well as modulated nitrogen basicity, which makes them one of the most promising moieties evaluated in structure−activity relationship (SAR) studies.[6−8] Not surprisingly, substituted morpholines are the fourth most common saturated scaffold found in FDA approved medicines, and they have a plethora of molecular targets.[9−14]

Many elegant reactions have been developed for the formation of substituted morpholine rings, including nucleophilic displacement,[15−17] ring expansion,[18−20] intramolecular[21−23] and intermolecular alkene cyclization,[24] and radical cyclization[25,26] (Figure 1a). Despite the utility of these methods, major drawbacks for many morpholine-forming reactions include the need for protecting groups on the nitrogen atom and the limitation of forming one stereogenic center. In addition, an in-depth analysis of recent diastereoselective routes for the preparation of morpholines containing two or more stereogenic centers reveals the paucity of methods to access certain important substitution patterns, such as 2,3-trans-substitution found in many medicinally valuable compounds (Figure 1b). For example, 2,3-disubstituted morpholines **2**−**4** are representative of this class of molecules that are being evaluated as lead compounds in drug discovery programs.[27−29]

The current state-of-the-art in diastereoselective morpholine synthesis is Bode's SnAP (stannyl amine protocol) and SLAP (silicon amine protocol) reactions, which avoid major limitations of other approaches (Figure 1a).[30,31] However, these strategies rely on reagents that are prefunctionalized with tin and silicon-based groups and require several steps to synthesize, which limits the types of functional groups (R^2 = Me, Et) and substitution patterns that can be incorporated into the morpholine products. A notable omission in the substrate scope of Bode's approaches is the synthesis of 2,3-disubstituted morpholines with high diastereoselectivity, which is necessary to access products such as **2**−**4**.[32] During the preparation of

Received: February 3, 2025
Revised: April 6, 2025
Accepted: April 7, 2025
Published: April 17, 2025

https://doi.org/10.1021/jacs.5c01832
J. Am. Chem. Soc. 2025, 147, 14605−14613

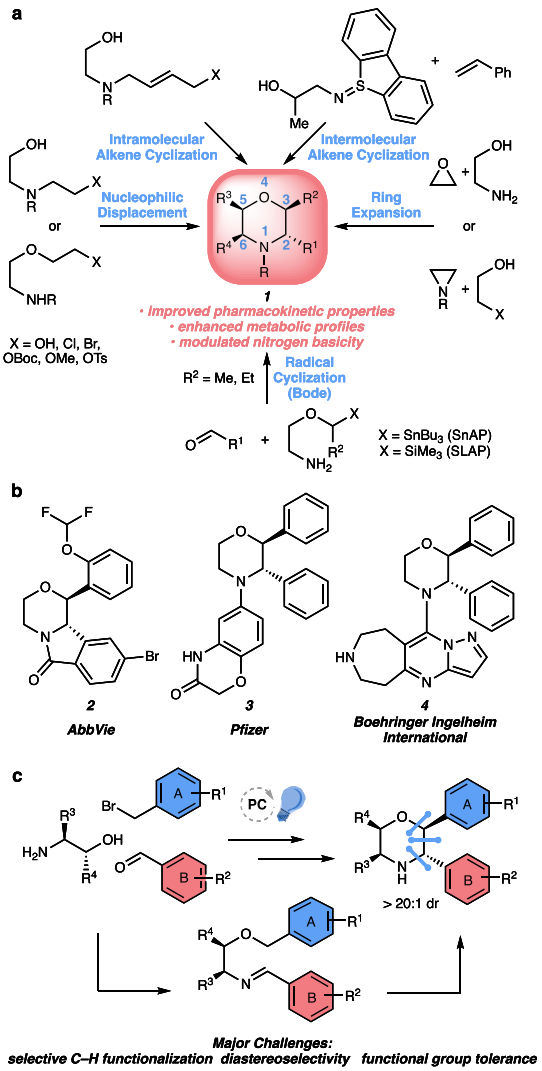

Figure 1. Strategies for Synthesizing Substituted Morpholines. (a) Current approaches for morpholine synthesis. (b) Selected examples of substituted morpholines for pharmaceutical applications. (c) Our synthesis of substituted morpholines via a photocatalytic C–H functionalization and annulation.

this manuscript, Nicewicz and co-workers reported an elegant photocatalytic synthesis of *N*-carbamoyl piperazines, a chemically distinct but equally important pharmacophore.[33]

Our goal was to develop a general and diastereoselective method to synthesize morpholines that would be amenable to a diverse range of substitution patterns and functional groups (Figure 1c). Herein, we demonstrate a modular approach to access functionalized morpholines with a variety of substitution patterns from readily available starting materials. This diastereoselective, photocatalytic C–H functionalization and annulation strategy enables rapid access to several functionalized and unprotected morpholines, and it represents a versatile disconnection for the assembly of complex morpholine scaffolds. We explore the scope of this method and provide mechanistic data. We also expand this mode of activation to the synthesis of other medicinally privileged *N*-heterocycles, such as piperidines and pyrrolidines.

RESULTS AND DISCUSSION

Reaction Development. We commenced our studies into the photocatalytic synthesis of morpholines by preforming imine **7a** via a neat condensation between 2-benzyloxy-1-ethanamine **5a** and benzaldehyde **6a** (Table 1). These conditions proved to be robust, as all imines in this study were quantitatively formed using this protocol.[34] With imine **7a** in hand, we began optimizing the annulation to form morpholine **8a** in the presence of a photocatalyst, a Brønsted acid (TfOH), and blue LED light. We first examined photocatalysts covering a range of excited-state reduction potentials. While acridinium catalysts[35,36] **A** ($E_{red}^{1/2}$* = +2.06 V vs SCE in CH_3CN) and **B** ($E_{red}^{1/2}$* = +2.15 V vs SCE in CH_3CN) provided the desired product in low yields (entries 1 and 2), in the presence of the more strongly photo-oxidizing 2,4,6-triphenylpyrylium tetrafluoroborate (TPP·BF_4) **C**[37] ($E_{red}^{1/2}$* = +2.39 V vs SCE in CH_3CN), morpholine **8a** was formed in 41% yield (entry 3).

Table 1. Optimization of Photocatalytic Morpholine Annulation[f]

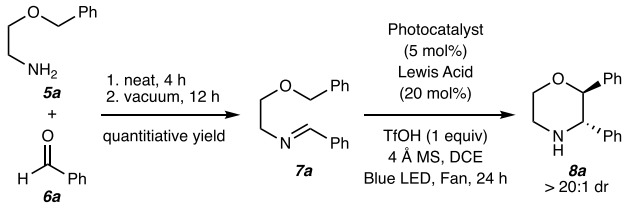

Entry	Photocatalyst	Lewis Acid	Yield (%)[a]
1	A	–	< 5
2	B	–	< 5
3	C	–	41
4	C	$Sn(OTf)_2$	12
5	C	$Cu(OTf)_2$	14
6	C	$CuBr_2$	40
7	C	$CuCl_2$	65
8	C	CuI	54
9	C	CuCl	84
10	C	CuBr	91 (91)[b]
11	–	CuBr	< 5
12[c]	C	CuBr	< 5
13[d]	C	CuBr	< 5
14[e]	C	CuBr	46

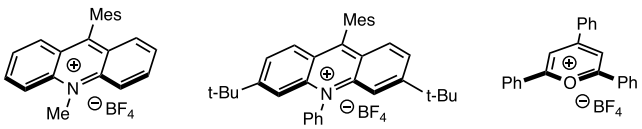

[a]NMR yield using 1,3,5-trimethoxybenzene as internal standard. [b]Isolated yield. [c]No light. [d]No TfOH. [e]No fan. [f]Reaction conditions: Imine **7a** (0.25 mmol, 1 equiv), Photocatalyst (5 mol %), Lewis Acid (20 mol %), TfOH (1 equiv), 4 Å MS (25 mg) in 1,2-dichloroethane (0.1 M). Blue LED strip lights.

https://doi.org/10.1021/jacs.5c01832
J. Am. Chem. Soc. 2025, 147, 14605–14613

Table 2. Substrate Scope of Photocatalytic Morpholine Annulation[c]

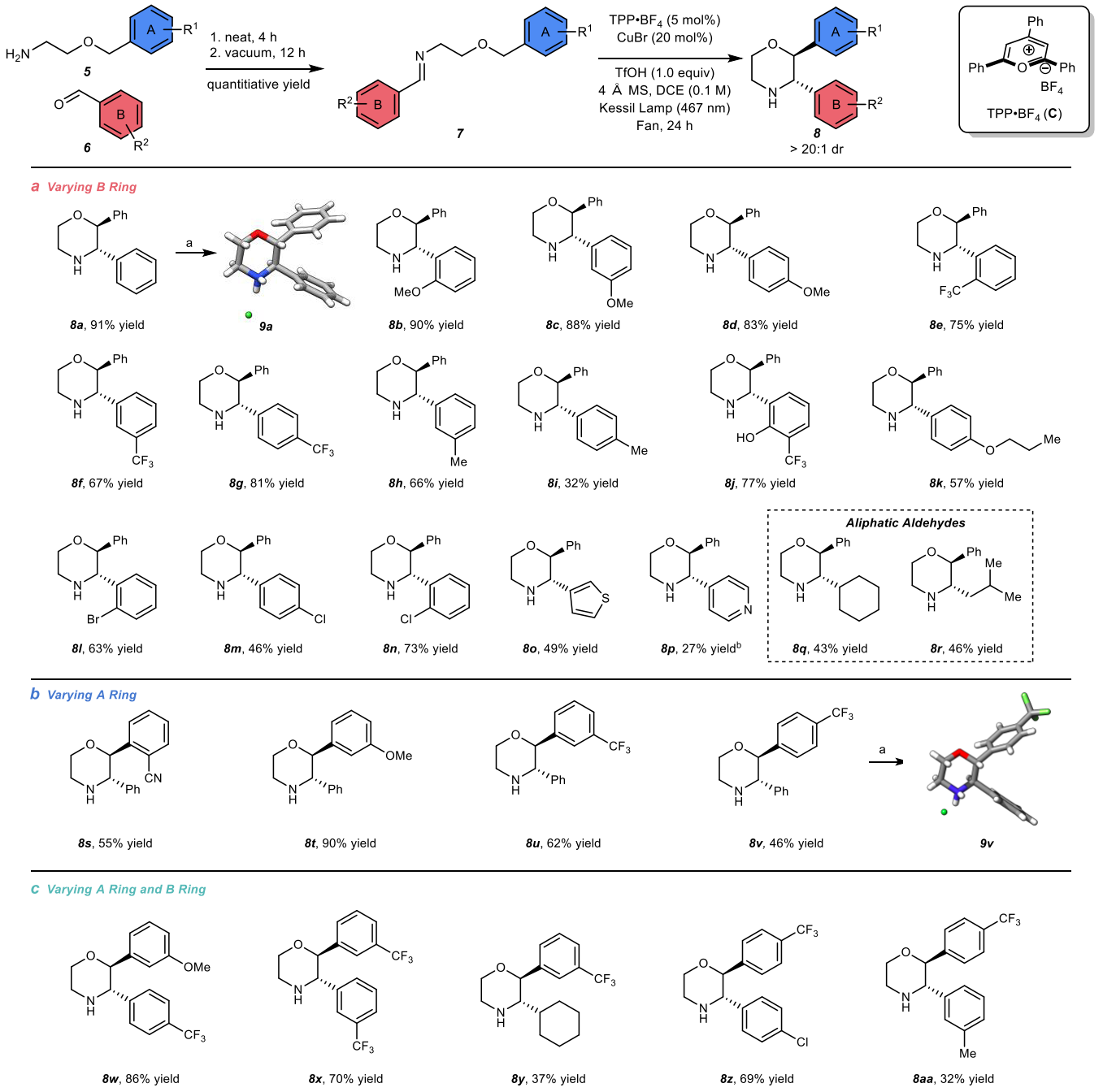

[a]4 M HCl in 1,4-dioxane, Et_2O (0.1 M), 23 °C. [b]Reaction performed on a 0.50 mmol scale. [c]Reaction conditions: Imine 7 (0.25 mmol, 1 equiv), Photocatalyst **C** (5 mol %), CuBr (20 mol %), TfOH (1 equiv), 4 Å MS (25 mg) in 1,2-dichloroethane (0.1 M).

Intrigued by recent developments in photocatalytic reactions aided by Lewis acid,[38−41] we examined the effects of various Lewis acids on the reaction efficiency (entries 4−10). While we did not observe a drastic yield improvement in the presence of $Sn(OTf)_2$ and several copper salts, CuBr provided 91% isolated yield of the desired morpholine **8a** (entry 10). Control experiments showed that the photocatalyst, light, and TfOH, were all required for annulation (entries 11−13). The presence of a fan was also important to achieve optimal conditions (entry 14). We believe this is due to the light source slowly heating the reaction vial over a 24 h period, leading to decomposition of the imine **7a** into amine and aldehyde starting materials, which was detected by ^{1}H NMR analysis.

Substrate Scope. With optimized conditions in hand, we examined the scope of the diastereoselective annulation with respect to the B ring at C2 of the morpholine (Table 2A). We started by assessing different electron withdrawing and donating groups around the B ring. *Ortho-*, *meta-*, and *para-*methoxy derivatives (**8b-8d**) were synthesized in 83−90% yield. Trifluoromethyl substituted imines (**8e−8g**) were also tested and resulted in yields ranging from 67 to 81%. In all cases, the diastereoselectivity was determined by ^{1}H NMR to be >20:1. The relative configuration of the major diastereomer

https://doi.org/10.1021/jacs.5c01832
J. Am. Chem. Soc. 2025, 147, 14605−14613

Table 3. Synthetic Utility of Photocatalytic Annulation

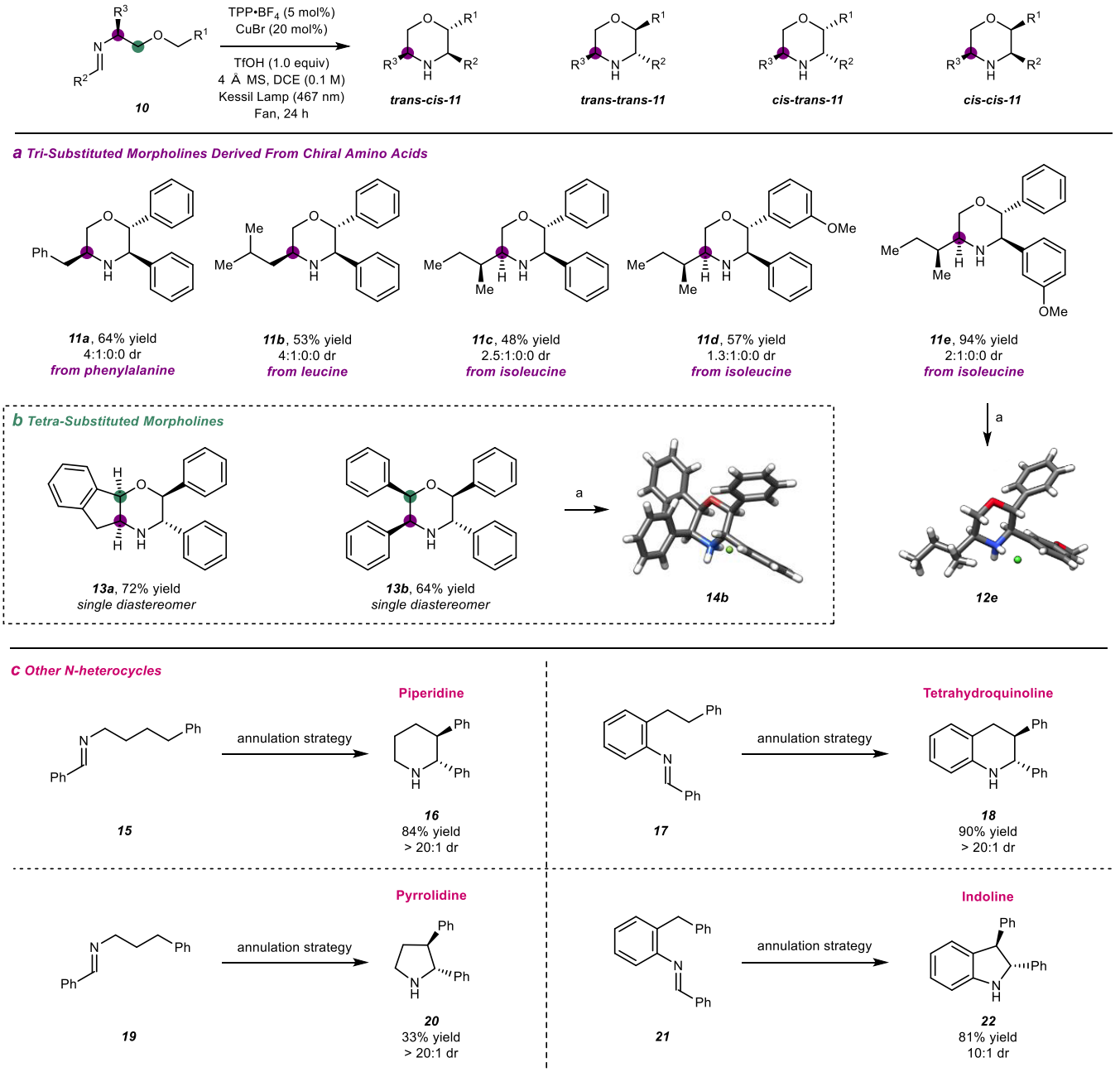

[a]4 M HCl in 1,4-dioxane, Et_2O (0.1 M), 23 °C.

of the product was determined to be *trans* by X-ray analysis of HCl salt **9a**, which was derived from morpholine **8a**. Other benzylic positions could also be introduced into the substrate, and we still observed activation of the C−H bond of the benzylic ether to form morpholines **8h** and **8i**. The comparatively lower yield of formation for morpholine **8i** may be due to competitive activation of the other benzylic C−H bond to yield undesired byproducts. Other functional groups such as phenols (**8j**), ethers (**8k**), and halogens like bromine (**8l**) and chlorine (**8m**, **8n**) were compatible with the transformation as well. Heteroaromatic aldehydes were tolerated in the transformation providing access to morpholines with thiophene (**8o**) and pyridine (**8p**) substituents. Aliphatic aldehydes also proved successful under these conditions, as we observed the formation of morpholines derived from cyclohexanecarboxaldehyde (**8q**) and isovaleraldehyde (**8r**).

We then examined the scope of the A ring at C3 of the morpholine (Table 2B). Electron donating groups such as methoxy were tolerated at the ortho position of the A ring, as morpholine **8t** was isolated in 90% yield. A *para*-methoxy substituent in the A ring led to decomposition of the imine, presumably because of its instability under the acidic reaction conditions. Electron withdrawing groups were also evaluated, as *ortho*-CN, *meta*-CF_3, and *para*-CF_3 groups provided the *trans* morpholine products (**8s, 8u-8v**). The relative stereochemistry of the major diastereomer of morpholine **8v** was confirmed by X-ray crystal analysis of the HCl salt, **9v**. When the A ring in the imine substrate was replaced with a simple methyl substituent, the 2-methyl morpholine product was not

https://doi.org/10.1021/jacs.5c01832
J. Am. Chem. Soc. 2025, 147, 14605−14613

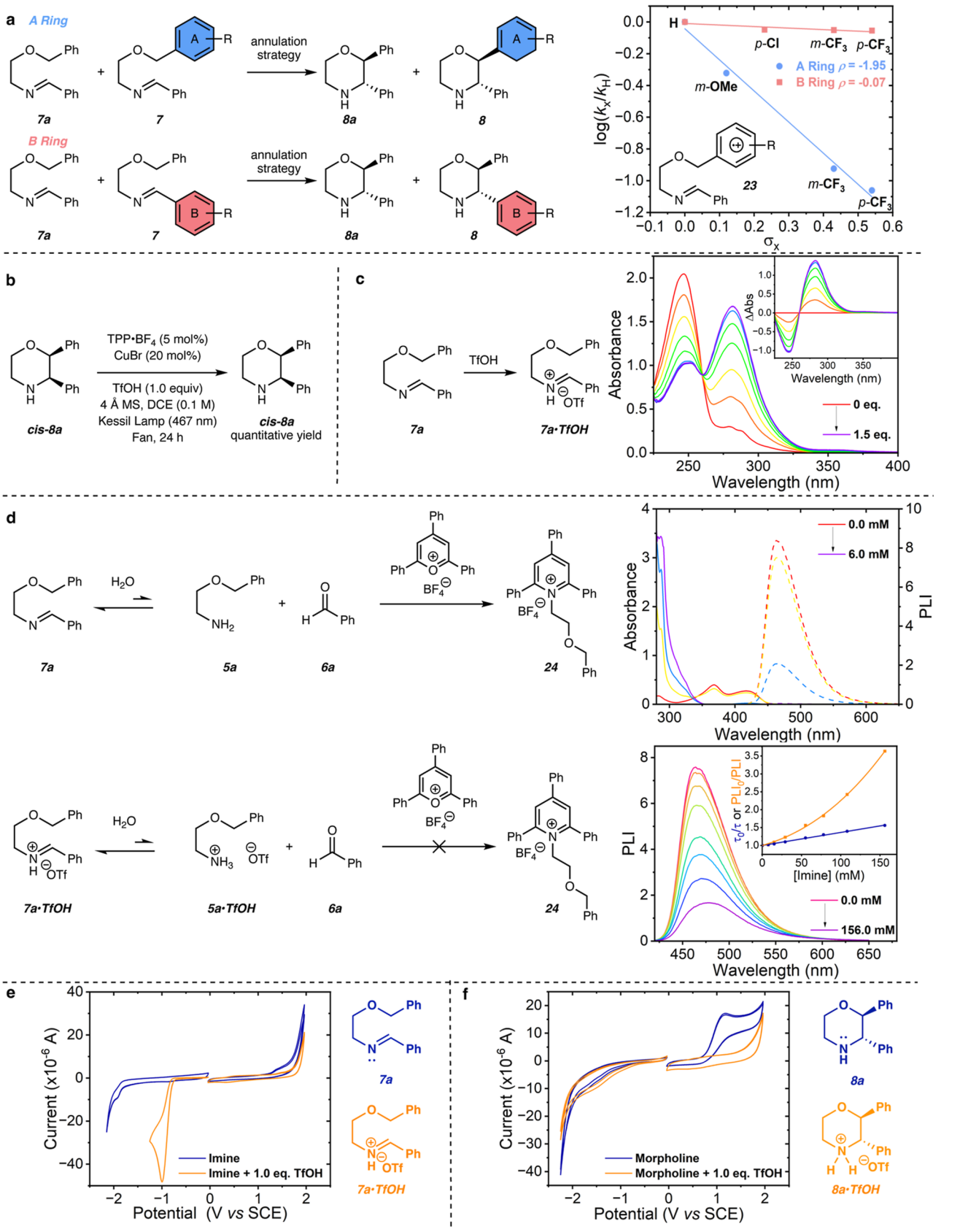

Figure 2. Mechanistic Studies on Photocatalytic Annulation. (a) Hammett plot identifies the rate-determining step as photo-oxidation of aromatic ring A. (b) Configurational stability of product under reaction conditions. (c) TfOH protonates imine. (d) TfOH prevents photocatalyst decomposition and allows efficient excited-state quenching. (e) TfOH affects the reduction potential of imine. (f) TfOH prevents product oxidation.

https://doi.org/10.1021/jacs.5c01832
J. Am. Chem. Soc. 2025, 147, 14605−14613

observed, which suggests the importance of the aromatic A ring in the mechanism of the reaction (vide infra).

We synthesized several 2,3-disubstituted morpholines in which both the A and B rings were substituted (**8w**−**8aa**). A combination of electron donating and withdrawing functional groups were incorporated to either ring system, and the *trans* morpholine products were generated in synthetically useful yields and >20:1 dr.

Morpholines from Amino Acids. We identified a unique opportunity to expand the synthetic utility of our morpholine annulation strategy by using enantiopure amino acids to generate the imine substrates **11** (Table 3a). This would not only enable the synthesis of trisubstituted morpholines but would also provide the opportunity to generate enantioenriched morpholine products. With the extra stereogenic center, we now had to overcome the challenge of forming 4 potential stereoisomers of morpholine **11** (*trans*−*cis*, *trans*−*trans*, *cis*−*trans*, and *cis*−*cis*).

We synthesized phenylalanine and leucine derived imines (see Supporting Information) and subjected them to our optimized reaction conditions. Gratifyingly, trisubstituted morpholines from phenylalanine and leucine (**11a**, **11b**) formed in good yields as a 4:1:0:0 mixture of stereoisomers, where the two *trans* diastereomers (relative to R^1 to R^2) were the only products observed. Isoleucine derived morpholine **11c** formed in 48% yield in a 2.5:1:0:0 ratio of stereoisomers, once again favoring the two *trans* isomers (relative to R^1 to R^2). Methoxy groups were incorporated in the *meta* positions of the A and B rings to further diversify the trisubstituted scaffold (**11d**, **11e**). Interestingly, the position of the methoxy substituent had a minor effect on the stereoselectivity of the reaction. The relative and absolute stereochemistry of the major stereoisomer of morpholine **11e** was confirmed by X-ray crystal analysis of the HCl salt, **12e**.

Tetrasubstituted Morpholines. We were excited to access tetra-substituted morpholines as well (Table 3b). Starting with an imine derived from (1*R*,2*S*)-(+)-*cis*-1-amino-2-indanol, we isolated tetracyclic scaffold **13a** in 72% yield as a single diastereomer. We also formed tetra-phenylmorpholine **13b** in 64% yield as a single diastereomer starting from (1*R*,2*S*)-(−)-2-amino-1,2-diphenylethanol. The relative stereochemistry of morpholine **13b** was confirmed by analysis of the X-ray crystal structure of its HCl salt, **14b**.

Beyond Morpholines. We hypothesized that our disconnection for the synthesis of morpholines via a photocatalytic C−H functionalization would be applicable to the synthesis of other medicinally privileged *N*-heterocycles (Table 3c). We generated a series of imines with remote benzylic C−H bonds. Under the optimized reaction conditions for morpholine synthesis, we generated an unprotected piperidine (**16**), tetrahydroquinoline (**18**), pyrrolidine (**20**), and indoline (**22**). The method was therefore accommodating of different ring sizes. In all cases, the *trans* diastereomer was generated with high diastereoselectivity.

Mechanistic Studies. To gain insight into the mechanism of the photocatalytic annulation, we first constructed Hammett plots to identify the rate-determining step of the reaction (Figure 2a). Competition experiments were performed between a series of substrates to measure the effect of aryl substitution on the rates of annulation. While substitution on the B ring had minimal effect on the reaction rate, substitution on the A ring had a more pronounced effect, with a ρ value of −1.95. The negative slope indicates a buildup of positive charge in the system,[42] suggesting that the rate-determining step of the reaction is the formation of radical cation intermediate **23** upon photochemical oxidation of the A ring.[43,44]

To ascertain whether the high diastereocontrol is due to selective formation of the *trans* isomer or epimerization of the *cis* isomer to the more thermodynamically stable *trans* isomer, the *cis* diastereomer of morpholine **8a** was independently synthesized (see Supporting Information) and resubjected to the reaction conditions (Figure 2b). After 24 h, morpholine *cis*-**8a** was reisolated in quantitative yields, suggesting that the high diastereoselectivity for *trans* morpholines is not due to a photocatalytic epimerization.[45]

Since TfOH was required for product formation (Table 1, entry 13), we were interested in understanding the role of this additive in the reaction mechanism. First, UV−vis titration experiments suggest that TfOH fully protonates imine **7a** to form the iminium ion **7a·TfOH**, as indicated by the presence of an isosbestic point at 260 nm (Figure 2c).

Second, we believe that protonation of imine **7a** also helps in preserving photocatalyst **C** under the reaction conditions (Figure 2d). In the absence of TfOH, Stern−Volmer quenching experiments between imine **7a** and photocatalyst **C** resulted in a nonlinear trend and a loss of color in the solution, which was consistent with a nonlight induced degradative process. We hypothesize that in the absence of TfOH, trace amounts of water can cause decomposition of imine **7a**, and the resulting amine **5a** could react with pyrylium photocatalyst **C** to form the corresponding Katritzky salt **24** (as observed by ^{1}H NMR). When Stern−Volmer quenching experiments were performed in the presence of a fixed concentration of TfOH, the solution remained colored and intense excited-state quenching of photocatalyst **C** was observed upon the addition of imine **7a**. Thus, the presence of TfOH helps in preventing deleterious pathways by forming the iminium ion **7a·TfOH** as well as protonating any trace amine **5a**, thereby preventing decomposition of the photocatalyst to the corresponding Katritzky salt **24**.

Third, cyclic voltammetry (CV) experiments suggest that TfOH may impact both the reduction potential of imine **7a** (Figure 2e) as well as the reduction potential of morpholine **8a** (Figure 2f). All CV studies were performed in the absence of copper salts, as they were not fully soluble in the reaction medium and they were also unnecessary for product formation (Table 1, entry 3). In the absence of TfOH, the electrochemical data recorded for imine **7a** does not show significant electrochemical waves between −2.0 and 2.0 V vs SCE. Upon addition of TfOH, a new reduction peak around −1.0 V was observed, which suggests that protonation of imine **7a** renders the single electron reduction of this substrate significantly easier. For morpholine **8a**, a nonreversible oxidation peak is observed in the absence of TfOH, which is most likely attributed to the oxidation to the morpholine radical cation. The lack of reversibility prevents the precise determination of the reduction potential of the morpholine/morpholine radical cation couple, but based on the electrochemical data, we estimate this potential to be around 1.2 V vs SCE. Upon addition of TfOH, the oxidation peak disappeared completely, implying that protonated morpholine **8a·TfOH** is recalcitrant to single electron oxidation (Figure 2f). Thus, TfOH could also help in protecting the final morpholine product toward light-induced oxidation from the excited photocatalyst **C**.

https://doi.org/10.1021/jacs.5c01832
J. Am. Chem. Soc. 2025, 147, 14605−14613

With these experiments in mind, we propose two possible mechanisms for the photocatalytic annulation (Figure 3).

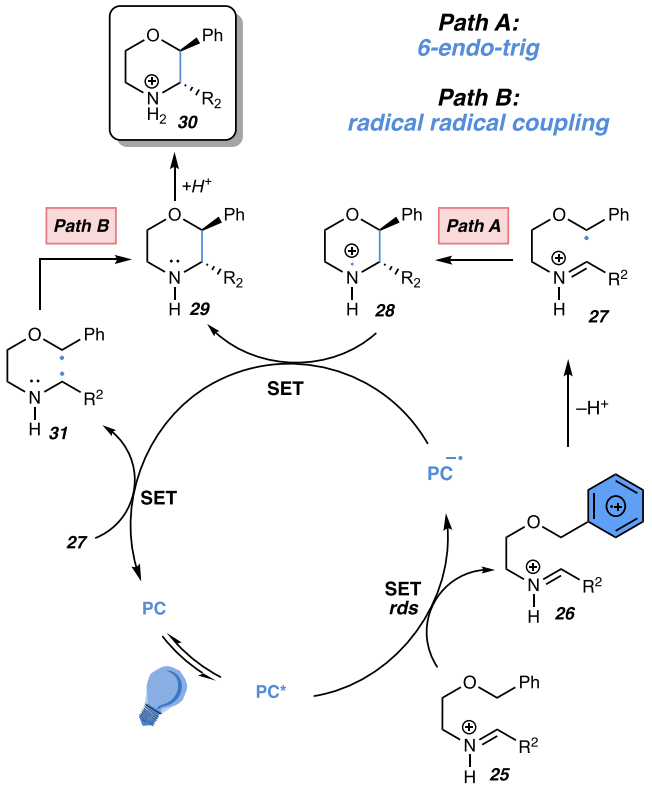

Figure 3. Proposed Mechanisms of Photocatalytic Annulation

Based on UV−vis titration studies, imine **7a** is protonated in the presence of TfOH to form iminium ion **25**. Both mechanistic paths commence with visible light activation of the photocatalyst to reach the corresponding excited state. The 4 ns excited-state lifetime of photocatalyst **C** is competent for bimolecular electron transfer with the iminium substrate, with the corresponding electron transfer rate constant of 1.2×10^9 M^{-1} s^{-1}. This charge-shift type reaction, confirmed by nanosecond UV−vis transient absorption spectroscopy (Figure S1), leads to the formation of the monoreduced photocatalyst and the oxidized radical cation **26** with a radical located on the A ring. Protonation of the imine with TfOH protects the imine from oxidation and thus enables oxidation of the A ring. Formation of oxidized radical cation **26** was revealed as the rate-determining step from Hammett plot analysis. This radical is then deprotonated to form benzylic radical **27**.

At this stage, two divergent mechanisms are proposed. In Path A, the benzylic radical adds into the iminium group via a 6-*endo-trig* cyclization to form nitrogen-based radical cation **28**. Subsequent single electron reduction results in morpholine **29** and the regenerated photocatalyst **C** to complete the catalytic cycle. Protonation of the morpholine with TfOH leads to intermediate **30**, which prevents undesired oxidation of the product, as described in Figure 2f.

In Path B, the iminium group in intermediate **27** undergoes a single electron reduction to form diradical **31** and the regenerated photocatalyst **C**. Radical−radical combination results in the formation of morpholine **29**, which is protonated by TfOH to provide the same final product as Path A. Based on our mechanistic studies, Path A is favored for three main reasons: (i) with a reduction potential of ∼1.2 V vs SCE (Figure 2f), the reduction of the nitrogen-based radical cation **28** by $PC^{\bullet-}$ ($E_{1/2}$ = − 0.35 V vs SCE) is thermodynamically favorable; (ii) the low concentration of radicals formed after photoinduced electron transfer would favor intramolecular 6-*endo-trig* cyclization over diffusional reactivity; and (iii) in Path B, the reduction of the iminium from $PC^{\bullet-}$ is uphill by ∼0.5 V (Figure 2e) and thus not thermodynamically favorable.

CONCLUSION

In summary, we have developed a robust diastereoselective annulation strategy to synthesize morpholines with various substitution patterns and functional groups. This method provides a novel way to build complex morpholine scaffolds from easily accessible starting materials. Additionally, the approach is extended to the synthesis of other valuable five- and six-membered *N*-heterocycles. Mechanistic studies unveil the rate-determining step of the reaction to be the formation of a radical cation on the A ring. Further mechanistic evaluation also suggests multiple roles of TfOH in the system, as it prevents decomposition of the photocatalyst and prevents product oxidation. We anticipate this general strategy will be amenable to many other cyclic scaffolds.

ASSOCIATED CONTENT

Supporting Information

The Supporting Information is available free of charge at https://pubs.acs.org/doi/10.1021/jacs.5c01832.

Experimental details, characterization data, and spectral data (PDF)

Accession Codes

Deposition Numbers 2380428−2380431 contain the supplementary crystallographic data for this paper. These data can be obtained free of charge via the joint Cambridge Crystallographic Data Centre (CCDC) and Fachinformationszentrum Karlsruhe Access Structures service.

AUTHOR INFORMATION

Corresponding Authors

Uttam K. Tambar − *Department of Biochemistry, The University of Texas Southwestern Medical Center, Dallas, Texas 75390-9038, United States;* orcid.org/0000-0001-5659-5355; Email: Uttam.Tambar@utsouthwestern.edu

Ludovic Troian-Gautier − *Institut de la Matière Condensée et des Nanosciences (IMCN), Molecular Chemistry, Materials and Catalysis (MOST), Université Catholique de Louvain (UCLouvain), 1348 Louvain-la-Neuve, Belgium; Wel Research Institute, 1300 Wavre, Belgium;* orcid.org/0000-0002-7690-1361; Email: Ludovic.Troian@uclouvain.be

Authors

Tiffany A. Brisco − *Department of Biochemistry, The University of Texas Southwestern Medical Center, Dallas, Texas 75390-9038, United States*

Simon De Kreijger − *Institut de la Matière Condensée et des Nanosciences (IMCN), Molecular Chemistry, Materials and Catalysis (MOST), Université Catholique de Louvain (UCLouvain), 1348 Louvain-la-Neuve, Belgium*

Vaishnavi N. Nair − *Department of Biochemistry, The University of Texas Southwestern Medical Center, Dallas, Texas 75390-9038, United States*

Complete contact information is available at:

https://pubs.acs.org/10.1021/jacs.5c01832

Author Contributions

The manuscript was written through contributions of all authors. All authors have given approval to the final version of the manuscript.

Notes

The authors declare no competing financial interest.

■ ACKNOWLEDGMENTS

L.T.-G. is a Chercheur Qualifié of the Fonds de la Recherche Scientifique—FNRS. L.T.-G. acknowledges support from the Fonds de la Recherche Scientifique (F.R.S.-FNRS) under grant CDR no. 40020332. L.T.-G. and S.D.K. acknowledge UCLouvain for financial support. The authors warmly acknowledge Prof. Benjamin Elias (and the corresponding U.N021.21 grant) for granting access to the nanosecond transient absorption apparatus. Financial support was provided to U.K.T by W. W. Caruth, Jr. Endowed Scholarship, Welch Foundation (I-1748), National Institutes of Health (R01GM102604), American Chemical Society Petroleum Research Fund (59177-ND1), and Teva Pharmaceuticals Marc A. Goshko Memorial Grant (60011-TEV). Financial support was provided to V.N.N. by the Sarah and Frank McKnight Fund Graduate Fellowship. We thank Eric Voight and Justin Dietrich from AbbVie for insightful conversations about the project. We also thank our unique group of lab members for creating an environment that supports our scientific endeavors. We acknowledge constructive discussions within the Catalysis Innovation Consortium, which facilitated this collaborative study.

■ REFERENCES

(1) Marshall, C. M.; Federice, J. G.; Bell, C. N.; Cox, P. B.; Njardarson, J. T. An Update on the Nitrogen Heterocycle Compositions and Properties of U.S. FDA-Approved Pharmaceuticals (2013−2023). *J. Med. Chem.* **2024**, *67* (14), 11622−11655.

(2) Wu, Y.-J. Chapter 1 - Heterocycles and Medicine: A Survey of the Heterocyclic Drugs Approved by the U.S. FDA from 2000 to Present. In *Progress in Heterocyclic Chemistry*; Gribble, G. W., Joule, J. A., Eds.; Elsevier, 2012; Vol. *24*, pp 1−53.

(3) *Asymmetric Synthesis of Nitrogen Heterocycles*; Royer, J., Ed.; Wiley-VCH Verlag GmbH & Co. KGaA, 2009.

(4) *New Methods for the Asymmetric Synthesis of Nitrogen Heterocycles, 2005*; Vicario, J. L., Badia, D., Carrillo, L., Eds.; Research Signpost, 2005.

(5) Naim, M. J.; Alam, O.; Alam, J. M.; Alam, P.; Shrivastava, N. A review on pharmacological profile of morpholine derivatives. *Int. J. Pharmacol. Pharm. Sci.* **2015**, *3*, 40−51.

(6) Tzara, A.; Xanthopoulos, D.; Kourounakis, A. P. Morpholine As a Scaffold in Medicinal Chemistry: An Update on Synthetic Strategies. *ChemMedChem* **2020**, *15* (5), 392−403.

(7) Kourounakis, A. P.; Xanthopoulos, D.; Tzara, A. Morpholine as a privileged structure: A review on the medicinal chemistry and pharmacological activity of morpholine containing bioactive molecules. *Med. Res. Rev.* **2020**, *40* (2), 709−752.

(8) Kumari, A.; Singh, R. K. Morpholine as ubiquitous pharmacophore in medicinal chemistry: Deep insight into the structure-activity relationship (SAR). *Bioorg. Chem.* **2020**, *96*, 103578.

(9) Lenci, E.; Calugi, L.; Trabocchi, A. Occurrence of Morpholine in Central Nervous System Drug Discovery. *ACS Chem. Neurosci.* **2021**, *12* (3), 378−390.

(10) Fukui, N.; Maki, T.; Ban, K.; Kijima, A.; Shibahara, S.; Okamoto, K.; Kamiya, S.; Yasukata, T.; Tsuritani, T. Practical Manufacturing Process for Baloxavir Marboxil: Efficient Route to a Tricyclic Triazinanone Scaffold. *Org. Process Res. Dev.* **2024**, *28* (6), 2128−2138.

(11) Pan, S.; Wu, X.; Jiang, J.; Gao, W.; Wan, Y.; Cheng, D.; Han, D.; Liu, J.; Englund, N. P.; Wang, Y.; et al. Discovery of NVP-LDE225, a Potent and Selective Smoothened Antagonist. *ACS Med. Chem. Lett.* **2010**, *1* (3), 130−134.

(12) Lamb, Y. N. Viloxazine: Pediatric First Approval. *Pediatric Drugs* **2021**, *23* (4), 403−409.

(13) Bouyssou, T.; Hoenke, C.; Rudolf, K.; Lustenberger, P.; Pestel, S.; Sieger, P.; Lotz, R.; Heine, C.; Büttner, F. H.; Schnapp, A.; et al. Discovery of olodaterol, a novel inhaled β2-adrenoceptor agonist with a 24h bronchodilatory efficacy. *Bioorg. Med. Chem. Lett.* **2010**, *20* (4), 1410−1414.

(14) Zarrinkar, P. P.; Gunawardane, R. N.; Cramer, M. D.; Gardner, M. F.; Brigham, D.; Belli, B.; Karaman, M. W.; Pratz, K. W.; Pallares, G.; Chao, Q.; et al. AC220 is a uniquely potent and selective inhibitor of FLT3 for the treatment of acute myeloid leukemia (AML). *Blood* **2009**, *114* (14), 2984−2992.

(15) Ortiz, K. G.; Brusoe, A. T.; An, J.; Chong, E.; Wu, L. Green Synthesis of Morpholines via Selective Monoalkylation of Amines. *J. Am. Chem. Soc.* **2024**, *146* (43), 29847−29856.

(16) Burg, F.; Rovis, T. Rh(III)-Catalyzed Intra- and Intermolecular 3,4-Difunctionalization of 1,3-Dienes via Rh(III)-π-Allyl Amidation with 1,4,2-Dioxazolones. *ACS Catal.* **2022**, *12* (15), 9690−9697.

(17) Matlock, J. V.; Svejstrup, T. D.; Songara, P.; Overington, S.; McGarrigle, E. M.; Aggarwal, V. K. Synthesis of 6- and 7-Membered N-Heterocycles Using α-Phenylvinylsulfonium Salts. *Org. Lett.* **2015**, *17* (20), 5044−5047.

(18) Singh, B.; Kumar, M.; Goswami, G.; Verma, I.; Ghorai, M. K. Ring-Opening Cyclization (ROC) of Aziridines with Propargyl Alcohols: Synthesis of 3,4-Dihydro-2H-1,4-oxazines. *J. Org. Chem.* **2023**, *88* (7), 4504−4518.

(19) Aubineau, T.; Cossy, J. A One-Pot Reaction toward the Diastereoselective Synthesis of Substituted Morpholines. *Org. Lett.* **2018**, *20* (23), 7419−7423.

(20) Ketan Das, B.; Sarkar, T.; Kumar Maharana, P.; Kar, S.; Punniyamurthy, T. Cascade Zinc- and Silver Catalyzed Stereospecific C−O and C−N Bond Formations. *Eur. J. Org Chem.* **2022**, *2022*, 251.

(21) Borah, M.; Borthakur, U.; Saikia, A. K. Diastereoselective Synthesis of Substituted Morpholines from N-Tethered Alkenols: Total Synthesis of (±)-Chelonin A. *J. Org. Chem.* **2017**, *82* (3), 1330−1339.

(22) Giofrè, S.; Molteni, L.; Nava, D.; Lo Presti, L.; Beccalli, E. M. Enantio- and Regioselective Palladium(II)-Catalyzed Dioxygenation of (Aza-)Alkenols. *Angew. Chem., Int. Ed.* **2021**, *60* (40), 21723−21727.

(23) Berhane, I. A.; Burde, A. S.; Kennedy-Ellis, J. J.; Zurek, E.; Chemler, S. R. Copper-catalyzed enantioselective alkene carboetherification for the synthesis of saturated six-membered cyclic ethers. *Chem. Commun.* **2021**, *57* (78), 10099−10102.

(24) Cheng, Q.; Bai, Z.; Tewari, S.; Ritter, T. Bifunctional sulfilimines enable synthesis of multiple N-heterocycles from alkenes. *Nat. Chem.* **2022**, *14* (8), 898−904.

(25) Luescher, M. U.; Bode, J. W. Catalytic Synthesis of N-Unprotected Piperazines, Morpholines, and Thiomorpholines from Aldehydes and SnAP Reagents. *Angew. Chem., Int. Ed.* **2015**, *54* (37), 10884−10888.

(26) Wang, Y.-Y.; Bode, J. W. Olefin Amine (OLA) Reagents for the Synthesis of Bridged Bicyclic and Spirocyclic Saturated N-Heterocycles by Catalytic Hydrogen Atom Transfer (HAT) Reactions. *J. Am. Chem. Soc.* **2019**, *141* (24), 9739−9745.

(27) Breinlinger, E. C.; Burchat, A.; Dietrich, J.; Friedman, M.; Ihle, D.; Kinsman, D.; Mullen, K.; Osuma, A.; Vasudevan, A.; Wilson, N. S. Indazolones as modulators of TNF signaling. U.S. Patent 10,273,238 B2, 2019.

(28) Casimiro-Garcia, A.; Futatsugi, K.; Piotrowski, D. W. Morpholine Compounds as Mineralocorticoid Receptor Antagonists. WO 2011141848 A1, 2011.

(29) Mueller, S.-G.; Brown, C. J.; Heifetz, A.; Nosse, B.; Prestle, J.; Prevost, N.; Rudolf, K.; Scheuerer, S.; Schindler, M.; Stenkamp, D.; Thomas, L.; Tye, H. 6,7,8,9-tetrahydro-5H-1,4,7,10a-tetraaza-cyclohepta[f]indene derivatives as 5-HT2C agonists. WO 2010060952 A1, 2010.
(30) Luescher, M. U.; Vo, C.-V. T.; Bode, J. W. SnAP Reagents for the Synthesis of Piperazines and Morpholines. *Org. Lett.* **2014**, *16* (4), 1236−1239.
(31) Jackl, M. K.; Legnani, L.; Morandi, B.; Bode, J. W. Continuous Flow Synthesis of Morpholines and Oxazepanes with Silicon Amine Protocol (SLAP) Reagents and Lewis Acid Facilitated Photoredox Catalysis. *Org. Lett.* **2017**, *19* (17), 4696−4699.
(32) Chu, D.; Zoll, A. J.; Ellman, J. A. Copper-Catalyzed Three-Component Synthesis of Highly Substituted Morpholines. *Org. Lett.* **2024**, *26* (22), 4803−4807.
(33) Boley, A. J.; Genova, J. C.; Nicewicz, D. A. Programmable Piperazine Synthesis via Organic Photoredox Catalysis. *J. Am. Chem. Soc.* **2024**, *146* (45), 31274−31280.
(34) Suzuki, S.; Ito, H.; Ishizuka, S.; Nonaka, R.; Noike, M.; Kodama, T.; Funaki, K.; Taguchi, M.; Kagaya, T.; Sato, S.; et al. Perfect solvent-and catalyst-free syntheses of imine derivatives using the pressure reduction technique. *Green Sustainable Chem.* **2019**, *09* (04), 105−118.
(35) Romero, N. A.; Margrey, K. A.; Tay, N. E.; Nicewicz, D. A. Site-selective arene C-H amination via photoredox catalysis. *Science* **2015**, *349* (6254), 1326−1330.
(36) Tlili, A.; Lakhdar, S. Acridinium Salts and Cyanoarenes as Powerful Photocatalysts: Opportunities in Organic Synthesis. *Angew. Chem., Int. Ed.* **2021**, *60* (36), 19526−19549.
(37) Miranda, M. A.; Garcia, H. 2,4,6-Triphenylpyrylium Tetrafluoroborate as an Electron-Transfer Photosensitizer. *Chem. Rev.* **1994**, *94* (4), 1063−1089.
(38) Narayanam, J. M. R.; Stephenson, C. R. J. Visible light photoredox catalysis: applications in organic synthesis. *Chem. Soc. Rev.* **2011**, *40* (1), 102−113.
(39) Prier, C. K.; Rankic, D. A.; MacMillan, D. W. C. Visible Light Photoredox Catalysis with Transition Metal Complexes: Applications in Organic Synthesis. *Chem. Rev.* **2013**, *113* (7), 5322−5363.
(40) Hopkinson, M. N.; Sahoo, B.; Li, J.-L.; Glorius, F. Dual Catalysis Sees the Light: Combining Photoredox with Organo-Acid, and Transition-Metal Catalysis. *Chem.—Eur. J.* **2014**, *20* (14), 3874−3886.
(41) Skubi, K. L.; Blum, T. R.; Yoon, T. P. Dual Catalysis Strategies in Photochemical Synthesis. *Chem. Rev.* **2016**, *116* (17), 10035−10074.
(42) Tanwar, L.; Börgel, J.; Ritter, T. Synthesis of Benzylic Alcohols by C−H Oxidation. *J. Am. Chem. Soc.* **2019**, *141* (45), 17983−17988.
(43) Hammett, L. P. The Effect of Structure upon the Reactions of Organic Compounds. Benzene Derivatives. *J. Am. Chem. Soc.* **1937**, *59* (1), 96−103.
(44) Hansch, C.; Leo, A.; Taft, R. W. A survey of Hammett substituent constants and resonance and field parameters. *Chem. Rev.* **1991**, *91* (2), 165−195.
(45) Shen, Z.; Vargas-Rivera, M. A.; Rigby, E. L.; Chen, S.; Ellman, J. A. Visible Light-Mediated, Diastereoselective Epimerization of Morpholines and Piperazines to More Stable Isomers. *ACS Catal.* **2022**, *12* (20), 12860−12868.

NOTE ADDED AFTER ASAP PUBLICATION

This article published ASAP on April 17, 2025. Tables 2 and 3 have been updated and the corrected version reposted the same day.

https://doi.org/10.1021/jacs.5c01832
J. Am. Chem. Soc. 2025, 147, 14605−14613